Density of states controls Anderson localization in disordered photonic crystal waveguides

P. D. García,[*] S. Smolka, S. Stobbe, and P. Lodahl[†]

DTU Fotonik, Department of Photonics Engineering, Technical University of Denmark, Ørsteds Plads 343,

DK 2800 Kongens Lyngby, Denmark

We prove Anderson localization in a disordered photonic crystal waveguide by measuring the ensemble-averaged extinction mean-free path, ℓ_e, which is controlled by the dispersion in the photon density of states (DOS) of the photonic crystal waveguide. Except for the very low DOS case, where out-of-plane losses are non-negligible, ℓ_e can be approximated to be the localization length ξ. The extinction mean-free path shows a fivefold variation between the low- and the high-DOS regime, and it becomes shorter than the sample length thus giving rise to strongly confined modes. The dispersive behavior of ℓ_e demonstrates the close relation between Anderson localization and the DOS in disordered photonic crystals, which opens a promising route to controlling and exploiting Anderson-localized modes for efficient light confinement.

PACS number(s): 42.25.Dd, 42.25.Fx, 42.70.Qs

Quantum optics and quantum information technologies require enhancement of light-matter interaction by, for example, confining light in a highly engineered nanocavity.[1] Quite remarkably, an alternative route toward light confinement exploits multiple scattering of light in disordered photonic structures, as originally proposed for electrons by Anderson.[2] The mechanism responsible for Anderson localization is wave interference and hence occurs not only for electrons but also for, e.g., microwaves,[3] acoustic waves,[4] and even Bose-Einstein condensated matter waves[5] thus illuminating the multidisciplinarity of the research field. In the case of light, indications of three-dimensional (3D) Anderson localization have been observed in random dielectric materials such as powders composed of particles with casual shapes and sizes.[6] In these systems no control can be exerted over the frequency or spatial extent of the localized modes.

A promising proposal on how to control multiple scattering is to induce slight amounts of disorder in periodic nanostructures called photonic crystals.[7] In an ideal photonic crystal the light propagation is described by Bloch modes. Breaking the symmetry of such structures leads to multiple scattering of light. The interference of multiply scattered light can lead to the formation of Anderson-localized modes appearing at random positions in the system but in a restricted frequency range close to the photonic crystal band gap. The modified photon density of states (DOS) in photonic crystals with respect to a homogenous material is expected not only to efficiently control the spontaneous emission of photons[8] but also to facilitate the strong localization of light.[9] The characteristic length scale of Anderson localization is the localization length ξ, which is the exponential decay length of the confined modes after averaging over many realizations of disorder. In one- and two-dimensional (1D, 2D) systems, localization occurs for any degree of disorder when the sample length exceeds ξ,[10] and the photonic conductor becomes an insulator. Contrary to nondispersive systems where localization cannot be controlled,[11] the modified DOS of a disordered photonic crystal controls Anderson localization through a highly dispersive ξ.

In this paper, we show experimentally how to control and accurately tune the localization length and the frequency range where Anderson-localized modes appear using disper-

sion in a photonic crystal. In particular, we use a 1D disordered photonic crystal waveguide (PCW) to measure the extinction mean-free path (MFP), ℓ_e, which describes the attenuation of the light transmission along the waveguide. By measuring a dispersive extinction MFP we confirm that the strongly confined modes appearing for high DOS in PCWs,[12] where we approximate $\ell_e \approx \xi$, are due to 1D Anderson localization, which has been questioned recently.[13] In addition, we interpret our experimental data of the wavelength-dependent localization length with a model for the DOS of a PCW thereby explicitly linking the localization length and the DOS. By doing so, we demonstrate the theoretically proposed relation between Anderson localization of light and the DOS. Indeed, photonic crystals owe their success to the fact that their DOS can be accurately tailored and we exploit this property to control Anderson localization.

Our samples consist of a membrane with a high refractive index material (GaAs, $n=3.54$) in which light is confined by total internal reflection. An ordered lattice of holes is etched in the structure forming a 2D photonic band gap that suppresses in-plane propagation of light. A waveguide is engineered in the structure by leaving out a row of holes. Light propagation in an ideal PCW is described by Bloch modes with a dispersion relation $\omega(k)$, where ω is the light wave frequency and k is the crystal wave number. The propagating mode on a PCW is susceptible to a strongly dispersive DOS defined as $\mathrm{DOS}=(1/\pi)\partial k/\partial \omega$. As a consequence, the group velocity of light can be slowed down since $v_g=1/(\pi \mathrm{DOS})$. Imperfections in a PCW lead to multiple scattering of light and the dispersion relation breaks down[14] thus inducing localized modes in the high-DOS regime if the sample length exceeds ξ.

To investigate the impact of disorder on the light propagation in PCW, we randomly vary the hole positions in the three nearest rows on each side of the waveguide using a Gaussian random number generator function (Box-Muller). The degree of disorder in each sample, δ, is characterized by the standard deviation of the hole position with respect to the lattice constant varying from $\delta=0\%$ to $\delta=12\%$ [Figs. 1(a) and 1(b)]. The samples consist of a triangular lattice of holes with a lattice constant $a=240$ nm, a filling fraction f
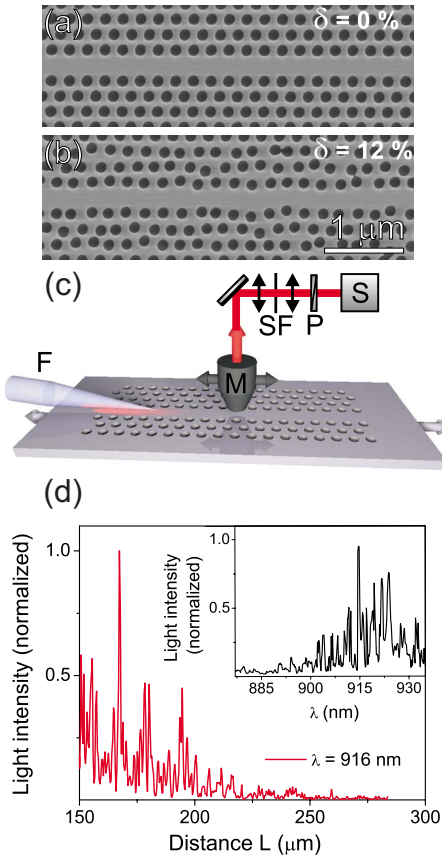
FIG. 1. (Color online) [(a) and (b)] Scanning electron microscope images of photonic crystal waveguides (top view) with engineered disorder on the positions of the holes of $\delta=0\%$ and $\delta=12\%$ (standard deviation relative to the lattice constant). (c) Setup used to measure the localization length. The tip of a single mode tapered fiber (F) is placed on the photonic crystal waveguide. TE-polarized light scattered from the waveguide is collected with an optical microscope objective (M), a spatial filter (SF), and a polarizer (P) and sent to a spectrometer (S) as a function of distance from the tapered fiber by moving the objective along the waveguide (indicated by the arrows at both sides of the objective). In order to repeat the measurement and perform ensemble average, we move the waveguide under the tapered fiber and microscope objective (indicated by the arrows at both ends of the waveguide). (d) Measurement of strongly fluctuating light intensity in the slow-light regime of a PCW with $\delta=0\%$ versus the distance from the light source. The inset of the figure shows a high-resolution (wavelength scan step size 0.1 nm) spectrum taken at $L=150$ μm from the fiber tip.

$=0.330\pm0.006$, membrane height $h=160\pm5$ nm, and a total length $L_0=1$ mm.

To characterize Anderson localization we use the optical setup illustrated in Fig. 1(c). A continuous-wave Ti:sapphire laser tunable within $\lambda=700-1000$ nm is coupled into a single mode tapered fiber with a tip diameter comparable to the waveguide width. The fiber evanescent mode couples to the waveguide mode by placing the fiber tip in close proximity of the PCW. We measure light scattered out of plane from the PCW with a high magnification microscope objective (NA=0.8) as a function of the wavelength (in step size of 1 nm) and the distance L from the fiber tip. The measure-

ment starts at $L=150$ μm from the fiber tip to avoid any spurious effect due to light that is not coupled to the waveguide mode. We note that any dependence of the in-coupling mechanism on the DOS would give rise to a dispersive out-of-plane scattered light intensity. However, this dependence is corrected by normalizing to the measurements at $L=150$ μm. The distance L is varied by scanning the microscope objective along the waveguide. Figure 1(d) shows a measurement for a single realization of disorder of scattered light intensity versus L for high DOS (at $\lambda=916$ nm where DOS>10 s nm^{-1}). In this case, $\delta=0\%$, the PCW is only affected by intrinsic unavoidable disorder introduced in the fabrication process. The inset of the figure shows a spectrum of the scattered light intensity at $L=150$ μm. The strong random fluctuation in the light intensity is a signature of 1D Anderson-localized modes. Since our waveguides do not have an abrupt termination (the wafer is not cleaved), these resonances are not Fabry-Perot type. The modes appear to be spatially and spectrally separated, which constitutes a criterion for Anderson localization.[15]

In the Anderson-localization regime, the fluctuating light transmission decays exponentially after ensemble averaging.[16] We assume that the scattered out-of-plane light intensity at a given position of the waveguide, I, is proportional to the total light intensity inside the sample, i.e., we assume that there is no significant spatial dependence of the out-of-plane scattering process. Any loss mechanisms of the light trapped in the PCW influences the measured decay length. In the presence of losses, we have $\langle\ln(I)\rangle=-L/\ell_{\rm e}$ where the extinction MFP, $\ell_{\rm e}$, is defined as

$$\ell_{\rm e}^{-1} = \ell_{\rm s}^{-1} + \ell_{\rm out}^{-1} + \ell_{\rm i}^{-1}, \tag{1}$$

where $\ell_{\rm s}$ is the scattering MFP associated with the backscattering process in the waveguide, $\ell_{\rm i}$ is the material inelastic absorption length, and $\ell_{\rm out}$ is the extinction length associated with out-of-plane losses. The relation $\xi\approx N\cdot\ell_{\rm s}$ holds for 1D systems,[16,17] where N is the number of electromagnetic modes that the system can sustain. Our samples are single-mode PCWs and hence the localization length is $\xi\approx\ell_{\rm s}$. We extract the extinction MFP by ensemble averaging the measured light leakage versus L and wavelength for eight different realizations of disorder. We probe different spatial realizations of disorder by moving the waveguide under the fiber and the microscope objective and repeating the measurement [see Fig. 1(c)]. Figure 2(a) shows the linear fit of $\langle\ln(I)\rangle$ along the waveguide with $\delta=0\%$ for low and high DOS (gray and black plot, respectively). In Fig. 2(b) we plot the DOS obtained from numerical simulations of the disorder-free ideal structure. For these spectral positions we extract the extinction MFP $\ell_{\rm e}(\lambda_1)=(161\pm16)$ μm and $\ell_{\rm e}(\lambda_2)=(30\pm2)$ μm.

Figure 2(c) shows the goodness of the fits, $\tilde{\chi}^2$, performed in Fig. 2(a) to test the degree of convergence of the ensemble average to a single-exponential decay. The fluctuations in the data are due to speckles not fully ensemble averaged. A
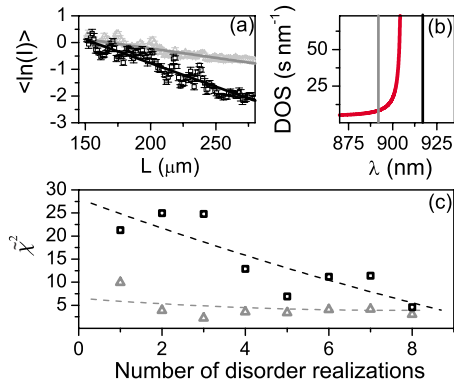
FIG. 2. (Color online) (a) Exponential fit of the ensemble-averaged light leakage intensity in PCWs with $\delta=0\%$ as a function of the distance from the source for two wavelengths: $\lambda_1=890$ nm (gray points) and $\lambda_2=916$ nm (black points). The spectral resolution is 2 nm and the slope equals the inverse of the extinction mean-free path. (b) The calculated DOS of an ideal structure without disorder. The two specific wavelengths λ_1 (gray line) and λ_2 (black line) are indicated that lie in the low- and high-DOS regimes, respectively. (c) Plot of the reduced chi square, $\tilde{\chi}^2$, for the exponential fit to the ensemble-averaged light transmission for low- (gray triangles) and high-DOS regime (black squares) versus number of realizations of disorder. The dashed lines are guide to the eyes.

single disorder realization in our experiment consists of a scan of $I(L)$ within a range of $150 < L < 280$ μm. Thus, the number of different disorder realizations that we can perform on one sample without adding repeated statistics to the ensemble average is limited by the sample length, $L_0=1$ mm. The goodness of the fit does not seem to level off at the optimum value $\tilde{\chi}^2=1$ that would prove the single-exponential model correct. Deviations from perfect verticality of the side walls of the air holes can break the symmetry in the out-of-plane direction and couple TE- and TM-polarized waveguide modes.[18] This polarization mixing mechanism may lead to multiexponential decay of the ensemble-averaged transmission that is not resolved in the present experiment.

Figure 3 contains the main contribution of this paper: it shows the dispersive behavior of the measured extinction MFP. We observe a fivefold variation in ℓ_e with wavelength. For very low DOS ($\lambda < 890$ nm), out-of-plane losses are predicted to dominate over backscattering losses in recent 3D numerical simulations of Bloch-mode scattering in PCWs.[19] Thus, we assume that ℓ_{out} becomes comparable to ξ in this spectral range, significantly affecting the measured extinction MFP. This is confirmed by the fact that pronounce intensity fluctuations are not observed in this spectral range (see inset of Fig. 1). For high DOS, on the contrary, the backscattering process is expected to dominate, and we attribute the variation in ℓ_e to a dispersive ξ. By assuming $\ell_e \cong \xi$ for high DOS, we observe how the localization length reaches its minimum value of $\sim(27 \pm 1)$ μm and becomes much smaller than L_0, giving rise to strongly localized modes. The dispersive behavior of the localization length gives directly control over the extension of the modes, which can be varied by tuning the wavelength. We can also carefully control the frequency range of the localized modes just
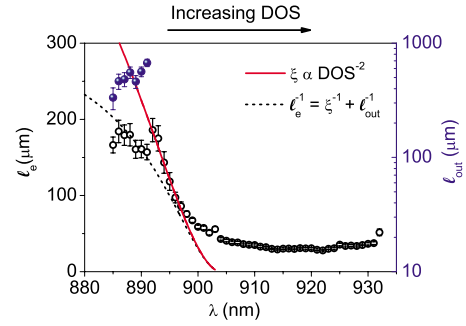

FIG. 3. (Color online) Plot of the extinction MFP, ℓ_e, of the PCW with $\delta=0\%$ as a function of the wavelength. A strongly dispersive extinction MFP is found that reaches a minimum for high DOS ($\lambda > 900$ nm). Losses mainly affect the extinction MFP for very low DOS ($\lambda < 890$ nm), where the length associated to out-of-plane losses (plotted as blue points) becomes comparable to the localization length. For higher DOS, the scaling $\xi \propto DOS^{-2}$ (red-continuous curve) is obtained from a model of the light scattering cross section in the PCW. The black-dashed curve is the fit to the data including wavelength-independent out-of-plane losses in the model.

by varying the fabrication parameters (typically a and f), thus, tuning the waveguide mode.

We now discuss the modeling of ξ. In our single-mode PCWs, the localization length is $\xi \approx \ell_s$. The dispersive behavior of ℓ_s in 3D photonic crystals has been measured and explained in terms of the DOS recently.[20] Two separate mechanisms determine ℓ_s: the excitation of the scatterer and the subsequent radiation from the scatterer.[21] The coupling to the scatterer is described by the DOS of the excitation beam,[22] i.e., the waveguide mode. The second process is described by the local DOS (LDOS). Ignoring the contributions of coupling to leaky radiation modes, the LDOS equals the DOS of the waveguide mode.[23,24] This applies to every scattering event giving rise to a modified scattering cross section σ in PCWs scaling as $\sigma \propto DOS^2(\omega)$. The scattering mean-free path in a random medium in the independent-scattering approximation can be expressed as $\ell_s = 1/\rho_s\sigma$,[25] where ρ_s is the density of scatterers. For 1D single-mode PCWs we therefore predict $\xi \propto DOS^{-2}(\omega)$, which is in good agreement with our experimental data for low DOS ($\lambda < 900$ nm). The red curve in Fig. 3 represents the best fit to our experimental results using the calculated DOS of the ideal photonic crystal structure [plotted in Fig. 2(b)]. The fitting parameters are the number of points fitted and the spectral position of the cutoff of the waveguide mode. The same scaling of $\xi \propto DOS^{-2}$ can also be recovered from 1D random matrix theory[26] and it is confirmed by 3D numerical simulations in PCWs.[19] It is also in agreement with single disorder realization measurements[27] and modeled with 1D perturbation theory.[28] From the data in Fig. 3 we observe that the model breaks down deep in the Anderson-localization regime ($\lambda > 900$ nm) where recurrent scattering occurs and the independent-scattering approximation is not valid anymore. The breakdown of our model may also be related to the fact that it is based on the calculated DOS of the ideal structure without disorder, which is modified in real structures.[29]
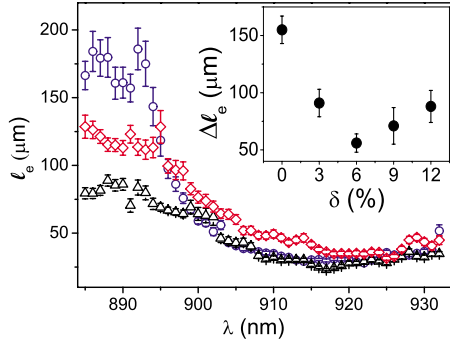
FIG. 4. (Color online) Extinction mean-free path, ℓ_e, as a function of wavelength measured in PCWs with various amounts of disorder $\delta = 0\%$ ($\bigcirc$), 6% ($\triangle$), and 12% ($\diamond$). The inset shows the difference between the maximum and minimum ℓ_e as a function of δ.

We observe that the experimental data depart from the model for very low DOS, which we attribute to non-negligible out-of-plane losses. In our case, GaAs has a very low optical-absorption coefficient (<100 cm^{-1} at a wavelength of $\lambda = 915$ nm) corresponding to $\ell_i > 1$ m. This value might be reduced by surface effects at the holes of the photonic crystal, but is still expected to be much larger than L_0, thus we ignore any absorption effect in our system. Therefore, the attenuation of the light transmission is only due to out-of-plane scattering and localization associated to back-scattering. Using Eq. (1), we extract ℓ_{out} from the difference between the modeled ξ (red curve in Fig. 3) and the measured ℓ_e. We note that this method for extracting ℓ_{out} assumes the validity of the model for ℓ_s with the limitations discussed above and is based on fitting two free parameters. Surprisingly, we observe an increase in ℓ_{out} with DOS (blue points in Fig. 3), which is in contrast to recent predictions.[19] Including a constant out-of-plane extinction length as a free parameter and a localization length $\xi \propto \text{DOS}^{-2}$ we fit the measured extinction MFP (black-dashed curve in Fig. 3). From the fit we obtain $\ell_{out} \sim 550$ μm, which is comparable to ξ for very low DOS. However, the model including a constant ℓ_{out} is not in good agreement to our data, which indicates a dispersive behavior also in the out-of-plane extinction length.

The effect of disorder on the extinction MFP is plotted in Fig. 4, which shows the measurement of ℓ_e in samples with increasing amount of disorder. The inset shows the difference between the maximum and minimum extinction MFP ($\Delta\ell_e$) occurring in the low- and high-DOS regime, respectively. It decreases with disorder, reaches a minimum for $\delta = 6\%$ and increases for $\delta > 6\%$. We explain the decrease in $\Delta\ell_e$ for weak disorder by an increase in the out-of-plane light losses, which is predicted in Ref. 19. The increase for $\delta > 6\%$ is surprising and reflects the complex interplay between dispersive out-of-plane losses and the disorder induced in the PCW. A similar behavior has been found in numerical investigations of disordered 3D photonic crystals in the absence of losses where an optimum amount of disorder was predicted,[30] which confirms the nontrivial relation between localization and disorder in PCs.
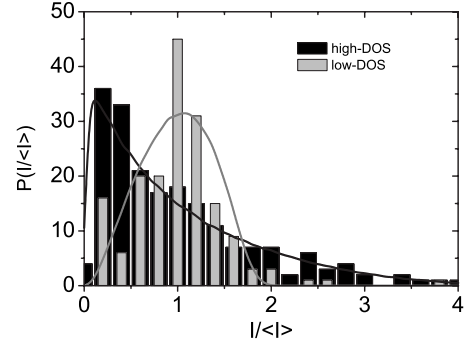

FIG. 5. Probability distributions of out-of-plane scattered light intensity in PCW with $\delta = 6\%$ for low and high DOS (gray and black histograms). Black and gray curves show the calculated probability distributions of intensity fluctuations with a 1D model of multiple scattering using sample length $L_0 = 250$ μm, out-of-plane extinction length $\ell_{out} = 260$ μm, and localization length $\xi = 90$ μm (high DOS) and $\xi = 230$ μm (low DOS), respectively.

Finally, we address the statistical properties of Anderson localization.[3] Figure 5 compares the probability distributions of out-of-plane scattered light intensity in PCW with $\delta = 6\%$ for low and high DOS (gray and black histograms, respectively). The normalized out-of-plane scattered light intensity, $I/\langle I \rangle$, is measured at a fixed distance from the fiber tip ($L_0 = 250$ μm) for ten different disorder realizations and varying the excitation wavelength in steps of 1 nm. In order to increase the statistics, we collect $I/\langle I \rangle$ at different wavelengths for low DOS, $\lambda = (885 \pm 10)$ nm and high DOS, $\lambda = (915 \pm 10)$ nm. For low DOS, we measure a Gaussian-type intensity distribution centered at $I/\langle I \rangle = 1$, which is expected when the sample length is comparable to the localization length. On the contrary, for high DOS the distribution broadens and the deviation from a Gaussian is pronounced. This behavior can only be observed for $\xi < \ell_{out}$.[31] The difference between the distributions for low and high DOS is a clear proof of a reduction in the localization length with DOS. To confirm this, we model our experimental distributions using transfer-matrix theory.[26] We obtain a good agreement by fitting our experimental distributions using a fixed sample length $L_0 = 250$ μm, a constant out-of-plane extinction length $\ell_{out} = 260$ μm, and two different localization lengths $\xi = 230$ μm and $\xi = 90$ μm for low and high DOS (gray and black-dashed curves in Fig. 5, respectively). We note that the intensity probability distributions do not provide a very precise way to distinguish between different values of the localization length and the out-of-plane extinction length since different sets of (ξ, ℓ_{out}) can give rise to very similar distributions and the experimental data are limited by finite statistics.

In conclusion, we have demonstrated the close relation between Anderson localization of light and the electromagnetic DOS in PCWs, which was theoretically predicted but not demonstrated experimentally. This close relationship allows us to accurately control the optical properties of

Anderson-localized modes appearing in the high-DOS regime of PCWs. We provide a method to fine tune the extension and frequency of these modes. These results are of fundamental importance since they impose limitations for traditional slow-light devices based on PCWs such as single-photon sources.[24] At the contrary the strongly confined Anderson-localized cavities with tailored properties open a new route to explore cavity quantum electrodynamics[32] or random lasing.

Note added. At this point, we would like to note that we became aware of a study of the transmission probability distributions in PCWs.[33] However, no account of the DOS-dependent localization length has been given.

*dgar@fotonik.dtu.dk

†pelo@fotonik.dtu.dk; http://www.fotonik.dtu.dk/quantumphotonics

[1] Y. Akahane, T. Asano, B. Song, and S. Noda, Nature (London) **425**, 944 (2003).

[2] P. W. Anderson, Phys. Rev. **109**, 1492 (1958).

[3] A. A. Chabanov, M. Stoytchev, and A. Z. Genack, Nature (London) **404**, 850 (2000).

[4] H. Hu, A. Strybulevych, J. H. Page, S. E. Skipetrov, and B. A. van Tiggelen, Nat. Phys. **4**, 945 (2008).

[5] J. Billy, V. Josse, Z. Zuo, A. Bernard, B. Hambrecht, P. Lugan, D. Clément, L. Sanchez-Palencia, P. Bouyer, and A. Aspect, Nature (London) **453**, 891 (2008); G. Roati, C. D'Errico, L. Fallani, M. Fattori, C. Fort, M. Zaccanti, G. Modugno, M. Modugno, and M. Inguscio, *ibid.* **453**, 895 (2008).

[6] D. S. Wiersma, P. Bartolini, A. Lagendijk, and R. Righini, Nature (London) **390**, 671 (1997); M. Störzer, P. Gross, C. M. Aegerter, and G. Maret, Phys. Rev. Lett. **96**, 063904 (2006).

[7] S. John, Phys. Rev. Lett. **58**, 2486 (1987).

[8] P. Lodahl, A. Floris van Driel, I. S. Nikolaev, A. Irman, K. Overgaag, D. Vanmaekelbergh, and W. L. Vos, Nature (London) **430**, 654 (2004).

[9] S. John and R. Rangarajan, Phys. Rev. B **38**, 10101 (1988).

[10] N. F. Mott and W. D. Twose, Adv. Phys. **10**, 107 (1961).

[11] J. Bertolotti, S. Gottardo, D. S. Wiersma, M. Ghulinyan, and L. Pavesi, Phys. Rev. Lett. **94**, 113903 (2005).

[12] J. Topolancik, B. Ilic, and F. Vollmer, Phys. Rev. Lett. **99**, 253901 (2007).

[13] M. Patterson, S. Hughes, S. Combrié, N.-V.-Quynh Tran, A. De Rossi, R. Gabet, and Y. Jaouën, Phys. Rev. Lett. **102**, 253903 (2009).

[14] N. Le Thomas, H. Zhang, J. Jágerská, V. Zabelin, R. Houdré, I. Sagnes, and A. Talneau, Phys. Rev. B **80**, 125332 (2009).

[15] D. J. Thouless, Phys. Rev. Lett. **39**, 1167 (1977).

[16] C. W. J. Beenakker, Rev. Mod. Phys. **69**, 731 (1997).

[17] A. García-Martín and J. J. Sáenz, Phys. Rev. Lett. **87**, 116603 (2001).

[18] J. Topolancik, F. Vollmer, R. Ilic, and M. Crescimanno, Opt. Express **17**, 12470 (2009).

[19] S. Mazoyer, J. P. Hugonin, and P. Lalanne, Phys. Rev. Lett. **103**, 063903 (2009).

[20] P. D. Garcia, R. Sapienza, L. S. Froufe-Perez, and C. Lopez, Phys. Rev. B **79**, 241109(R) (2009).

[21] L. S. Froufe-Perez, R. Sapienza, P. D. Garcia, and C. Lopez (unpublished).

[22] R. C. McPhedran, L. C. Botten, J. McOrist, A. A. Asatryan, C. M. de Sterke, and N. A. Nicorovici, Phys. Rev. E **69**, 016609 (2004).

[23] V. S. C. Manga Rao and S. Hughes, Phys. Rev. B **75**, 205437 (2007).

[24] T. Lund-Hansen, S. Stobbe, B. Julsgaard, H. Thyrrestrup, T. Sünner, M. Kamp, A. Forchel, and P. Lodahl, Phys. Rev. Lett. **101**, 113903 (2008).

[25] P. Sheng, *Introduction to Wave Scattering, Localization, and Mesoscopic Phenomena* (Academic Press, San Diego, 1995).

[26] L. S. Froufe-Pérez, M. Yépez, P. A. Mello, and J. J. Sáenz, Phys. Rev. E **75**, 031113 (2007).

[27] E. Kuramochi, M. Notomi, S. Hughes, A. Shinya, T. Watanabe, and L. Ramunno, Phys. Rev. B **72**, 161318(R) (2005); R. J. P. Engelen, D. Mori, T. Baba, and L. Kuipers, Phys. Rev. Lett. **101**, 103901 (2008); L. O'Faolain, T. P. White, D. O'Brien, X. Yuan, M. D. Settle, and T. F. Krauss, Opt. Express **15**, 13129 (2007).

[28] S. Hughes, L. Ramunno, J. F. Young, and J. E. Sipe, Phys. Rev. Lett. **94**, 033903 (2005).

[29] H. Thyrrestrup, L. Sapienza, and P. Lodahl, Appl. Phys. Lett. **96**, 231106 (2010).

[30] C. Conti and A. Fratalocchi, Nat. Phys. **4**, 794 (2008).

[31] S. A. van Langen, P. W. Brouwer, and C. W. J. Beenakker, Phys. Rev. E **53**, R1344 (1996).

[32] L. Sapienza, H. Thyrrestrup, S. Stobbe, P. D. Garcia, S. Smolka, and P. Lodahl, Science **327**, 1352 (2010).

[33] S. Mazoyer, P. Lalanne, J. C. Rodier, J. P. Hugonin, M. Spasenović, L. Kuipers, D. M. Beggs, and T. F. Krauss, Opt. Express **18**, 14654 (2010).